SIAM J. NUMER. ANAL.
Vol. 58, No. 5, pp. 2915–2933

A PRESSURE-ROBUST EMBEDDED DISCONTINUOUS GALERKIN METHOD FOR THE STOKES PROBLEM BY RECONSTRUCTION OPERATORS*

PHILIP L. LEDERER† AND SANDER RHEBERGEN‡

Abstract. The embedded discontinuous Galerkin (EDG) finite element method for the Stokes problem results in a pointwise divergence-free approximate velocity on cells. However, the approximate velocity is not $H(\mathrm{div})$-conforming, and it can be shown that this is the reason that the EDG method is not pressure-robust, i.e., the error in the velocity depends on the continuous pressure. In this paper we present a local reconstruction operator that maps discretely divergence-free test functions to exactly divergence-free test functions. This local reconstruction operator restores pressure-robustness by only changing the right-hand side of the discretization, similar to the reconstruction operator recently introduced for the Taylor–Hood and mini elements by Lederer et al. [*SIAM J. Numer. Anal.*, 55 (2017), pp. 1291–1314]. We present an a priori error analysis of the discretization showing optimal convergence rates and pressure-robustness of the velocity error. These results are verified by numerical examples. The motivation for this research is that the resulting EDG method combines the versatility of discontinuous Galerkin methods with the computational efficiency of continuous Galerkin methods and accuracy of pressure-robust finite element methods.

Key words. Stokes equations, embedded, discontinuous Galerkin finite element methods, pressure-robustness, exact divergence-free velocity reconstruction

AMS subject classifications. 65N12, 65N15, 65N30, 76D07, 76M10

DOI. 10.1137/20M1318389

1. Introduction.

Changing the body force of the continuous Stokes equations by a gradient field changes only the pressure solution, not the velocity. A finite element method for the Stokes equations that mimics this property at the discrete level is called *pressure-robust* and results in an a priori error estimate for the velocity that does not depend on the pressure error scaled by the inverse of the viscosity. The significance of this result is that large errors in the pressure, as may occur, for example, in natural convection problems, do not affect the velocity [17].

A finite element for the Stokes equations that is both conforming and divergence-free is pressure-robust [12, 13, 36]. These finite element methods, however, are generally difficult to implement, and traditional finite element methods often relax one, or both, of these conditions. Unfortunately, the resulting method is often not pressure-robust. It was observed in [26, 27] that this is due to a lack of L^2-orthogonality between irrotational and discretely divergence-free vector fields. In [27] L^2-orthogonality between irrotational and discretely divergence-free vector fields is restored for the first-order Crouzeix–Raviart element [7] by replacing discretely divergence-free vector fields by divergence-free lowest-order Raviart–Thomas [3] velocity reconstructions

*Received by the editors February 12, 2020; accepted for publication (in revised form) July 27, 2020; published electronically October 14, 2020.
https://doi.org/10.1137/20M1318389
Funding: The work of the first author was supported by the Austrian Science Fund (FWF) through the research program "Taming complexity in partial differential systems" (F65) and the project "Automated discretization in multiphysics" (P10). The work of the second author was supported by the Natural Sciences and Engineering Research Council of Canada (NSERC) Discovery grant RGPIN-05606-2015.
†Institute for Analysis and Scientific Computing, TU Wien, Vienna, Austria (philip.lederer@tuwien.ac.at).
‡Department of Applied Mathematics, University of Waterloo, Canada (srheberg@uwaterloo.ca).

wherever L^2 scalar products occur in the momentum balance equations. This simple modification (for the Stokes equations only the right-hand side of the discretization needs to be modified locally) results in a pressure-robust first-order Crouzeix–Raviart discretization of the (Navier–)Stokes equations. For discretizations of the (Navier–)Stokes equations using a "discontinuous" pressure approximation this modification is generalized to nonconforming and conforming mixed finite elements of arbitrary order in [28, 29] and to virtual finite element methods in [8]. Pressure-robustness is restored for the Taylor–Hood [15] and mini elements [1], which have "continuous" pressure approximations, in [22].

An alternative to the above-mentioned modification of traditional finite element methods is to use $H(\mathrm{div})$-conforming discontinuous Galerkin (DG) methods [6, 18]. $H(\mathrm{div})$-conforming DG discretizations are not only (automatically) pressure-robust; they are also ideally suited for convection dominated flows due to the natural incorporation of upwinding at element boundaries.

Unfortunately, DG methods are known to be computationally expensive. Hybridizable DG (HDG) methods were introduced to address this issue [5]. This is achieved by introducing new trace unknowns. The governing equations are then posed cellwise in terms of the approximate fields on a cell and numerical fluxes. The numerical fluxes are defined in terms of the traces of the approximate fields on the cell and the new trace unknowns in such a way that the approximate fields defined on a cell communicate only to fields that are defined on facets. This definition of the numerical flux allows cheap elimination of all cell degrees of freedom (DOFs), significantly reducing the number of globally coupled DOFs. Recent years have seen the development of many $H(\mathrm{div})$-conforming HDG methods [9, 25, 31] which, like the $H(\mathrm{div})$-conforming DG methods, are (automatically) pressure-robust. To reduce the number of coupled DOFs even further, $H(\mathrm{div})$-conformity was introduced only in a relaxed manner in [22, 23]. Finally, we want to mention the work in [11, 10, 21] where the authors derived a mixed method with $H(\mathrm{div})$-conforming velocities.

The $H(\mathrm{div})$-conforming HDG method in [31] introduces *discontinuous* trace velocity and trace pressure approximations. An alternative is to use *continuous* trace velocity and *discontinuous* trace pressure approximations. This results in the recently introduced embedded-hybridized DG (EDG-HDG) method [33]. The $H(\mathrm{div})$-conforming EDG-HDG method has even less globally coupled DOFs than an HDG method due to the use of a continuous trace velocity approximation. It is possible to lower the number of globally coupled DOFs even further by using both continuous trace velocity and trace pressure approximations. The resulting method is known as an embedded DG (EDG) method and was introduced for the Navier–Stokes equations in [19, 20]. It was demonstrated in [33], using the preconditioner of [32], that CPU time and iteration count to convergence is significantly reduced using continuous trace approximations compared to using discontinuous trace approximations (HDG method). Unfortunately, the EDG method is not pressure-robust.

In this paper we restore pressure-robustness of the EDG discretization of the Stokes equations [20, 30]. As with the HDG method, cell DOFs can be eliminated cheaply resulting in a global system only for the velocity and pressure trace approximations. Due to the continuity of the pressure trace approximation we follow a similar approach as presented in [24] to restore pressure-robustness. Therein a reconstruction operator for weakly divergence-free velocities was defined which was based on solving local problems on vertex patches. This local approach was motivated by the lifting techniques introduced for equilibrated error estimators [4]. In contrast to [24], where the reconstruction operator was used to eliminate the local divergence on each cell, the reconstruction operator in this work only enforces exact normal continuity since the EDG solution is already exactly divergence-free on a cell.

This paper is organized as follows. We present the EDG method for the Stokes problem in section 2. Section 3 presents the main result of this paper: a reconstruction operator to restore pressure-robustness of the EDG method and an a priori error analysis. Numerical examples to support our theory are presented in section 4, and conclusions are drawn in section 5.

2. The EDG method. In this section we present the EDG method for the Stokes problem. We introduce the approximation spaces and the discrete problem and discuss some properties of the discrete Stokes problem.

2.1. The Stokes problem. Let $\Omega \subset \mathbb{R}^{\dim}$ be a polygonal ($\dim = 2$) or polyhedral ($\dim = 3$) domain, and let $\partial\Omega$ denote its boundary. The Stokes problem is given by the following: find the velocity $u : \Omega \to \mathbb{R}^{\dim}$ and (kinematic) pressure $p : \Omega \to \mathbb{R}$ such that

$$-\nu\nabla^2 u + \nabla p = f \qquad \text{in } \Omega, \tag{2.1a}$$

$$\nabla \cdot u = 0 \qquad \text{in } \Omega, \tag{2.1b}$$

$$u = 0 \qquad \text{on } \partial\Omega, \tag{2.1c}$$

$$\int_\Omega p \, \mathrm{d}x = 0, \tag{2.1d}$$

where $f : \Omega \to \mathbb{R}^{\dim}$ is a given body force and $\nu \in \mathbb{R}^+$ is the kinematic viscosity.

2.2. Notation. To discretize the Stokes problem (2.1) by the EDG method, we first introduce a triangulation $\mathcal{T} := \{K\}$ of Ω consisting of nonoverlapping cells K. We denote the boundary of a cell K by ∂K and the outward unit normal vector on ∂K by n. The diameter of a cell K is denoted by h_K, and we define $h := \max_{K\in\mathcal{T}} h_K$. Two adjacent cells K^+ and K^- share an interior facet F, while a boundary facet is part of ∂K that lies on the domain boundary $\partial\Omega$. The set of all facets is denoted by $\mathcal{F} := \{F\}$. We denote the union of all facets by Γ^0.

We require the following approximation spaces:

$$V_h := \left\{ v_h \in [L^2(\Omega)]^{\dim} \ : \ v_h \in \left[P_k(K)\right]^{\dim} \ \forall K \in \mathcal{T} \right\}, \tag{2.2a}$$

$$Q_h := \left\{ q_h \in L^2(\Omega) \ : \ q_h \in P_{k-1}(K) \ \forall K \in \mathcal{T} \right\} \cap L^2_0(\Omega), \tag{2.2b}$$

$$\bar{V}_h^d := \left\{ \bar{v}_h \in [L^2(\Gamma^0)]^{\dim} \ : \ \bar{v}_h \in \left[P_k(F)\right]^{\dim} \ \forall F \in \mathcal{F}, \ \bar{v}_h = 0 \text{ on } \partial\Omega \right\}, \tag{2.2c}$$

$$\bar{Q}_h^{m,d} := \left\{ \bar{q}_h \in L^2(\Gamma^0) \ : \ q_h \in P_m(F) \ \forall F \in \mathcal{F} \right\}, \tag{2.2d}$$

where $P_k(K)$ and $P_k(F)$ denote the set of polynomials of degree k on a cell K and on a facet F, respectively, and where $L^2_0(\Omega) := \{q \in L^2(\Omega) \ : \ \int_\Omega q \, \mathrm{d}x = 0\}$. In this manuscript we consider both the case where $m = k-1$ (for $k \geq 2$) and the case where $m = k$ (for $k \geq 1$).

We next impose continuity of the "facet" spaces,

$$\bar{V}_h := \bar{V}_h^d \cap \left[C^0(\Gamma^0)\right]^{\dim} \quad \text{and} \quad \bar{Q}_h^m := \bar{Q}_h^{m,d} \cap C^0(\Gamma^0), \tag{2.3}$$

and define $\boldsymbol{V}_h := V_h \times \bar{V}_h$ and $\boldsymbol{Q}_h^m := Q_h \times \bar{Q}_h^m$. Function pairs in $\boldsymbol{V}_h$ and $\boldsymbol{Q}_h^m$ are denoted by $\boldsymbol{v}_h := (v_h, \bar{v}_h) \in \boldsymbol{V}_h$ and $\boldsymbol{q}_h := (q_h, \bar{q}_h) \in \boldsymbol{Q}_h^m$. For notational purposes we will drop the superscript m in the definition of the pressure space for the remainder of this paper if a result holds for both $m = k-1$ and $m = k$.

To discuss properties of the discrete Stokes problem we require the following extended function spaces:

$$V(h) := V_h + \left[H_0^1(\Omega)\right]^{\dim} \cap \left[H^2(\Omega)\right]^{\dim}, \qquad Q(h) := Q_h + L_0^2(\Omega) \cap H^1(\Omega),$$
$$\bar{V}(h) := \bar{V}_h + [H_0^{3/2}(\Gamma_0)]^{\dim}, \qquad \bar{Q}(h) := \bar{Q}_h + H_0^{1/2}(\Gamma_0).$$

We define on $V(h) \times \bar{V}(h)$ the mesh-dependent norms

(2.4)
$$|||\boldsymbol{v}|||_1^2 := \sum_{K\in\mathcal{T}} \|\nabla v\|_K^2 + \sum_{K\in\mathcal{T}} \frac{\alpha_v}{h_K}\|\bar{v} - v\|_{\partial K}^2, \qquad |||\boldsymbol{v}|||_{1,*}^2 := |||\boldsymbol{v}|||_*^2 + \sum_{K\in\mathcal{T}} \frac{h_K}{\alpha}\left\|\frac{\partial v}{\partial n}\right\|_{\partial K}^2$$

and remark that the norms $|||\cdot|||_1$ and $|||\cdot|||_{1,*}$ are equivalent on the finite element space $\boldsymbol{V}_h$. On $Q(h) \times \bar{Q}(h)$ we introduce the norm

$$|||\boldsymbol{q}|||_Q^2 := \|q\|_\Omega^2 + \|\bar{q}\|_Q^2, \tag{2.5}$$

where $\|\bar{q}\|_Q^2 := \sum_{K\in\mathcal{T}} h_K \|\bar{q}\|_{\partial K}^2$.

2.3. Definition and properties of the discrete Stokes problem. The EDG method for the Stokes problem (2.1) is given by [33]: find $(\boldsymbol{u}_h, \boldsymbol{p}_h) \in \boldsymbol{V}_h \times \boldsymbol{Q}_h$ such that

$$a_h(\boldsymbol{u}_h, \boldsymbol{v}_h) + b_h(\boldsymbol{p}_h, v_h) = \int_\Omega f \cdot v_h \,\mathrm{d}x \qquad \forall \boldsymbol{v}_h \in \boldsymbol{V}_h, \tag{2.6a}$$
$$b_h(\boldsymbol{q}_h, u_h) = 0 \qquad \forall \boldsymbol{q}_h \in \boldsymbol{Q}_h, \tag{2.6b}$$

where $a_h(\cdot,\cdot)$ defined on $(V(h)\times\bar{V}(h))\times\boldsymbol{V}_h$ and $b_h(\cdot,\cdot)$ defined on $(Q(h)\times\bar{Q}(h))\times V(h)$ are given by

$$\begin{aligned} a_h(\boldsymbol{u}, \boldsymbol{v}) := {} & \sum_{K\in\mathcal{T}} \int_K \nu \nabla u : \nabla v \,\mathrm{d}x + \sum_{K\in\mathcal{T}} \int_{\partial K} \frac{\nu\alpha}{h_K}(u - \bar{u})\cdot(v - \bar{v})\,\mathrm{d}s \\ & - \sum_{K\in\mathcal{T}} \int_{\partial K} \nu \left[(u - \bar{u})\cdot \tfrac{\partial v}{\partial n} + \tfrac{\partial u}{\partial n}\cdot(v - \bar{v})\right]\mathrm{d}s, \end{aligned} \tag{2.7a}$$
$$b_h(\boldsymbol{p}, v) := -\sum_{K\in\mathcal{T}} \int_K p\nabla\cdot v\,\mathrm{d}x + \sum_{K\in\mathcal{T}} \int_{\partial K} v\cdot n\bar{p}\,\mathrm{d}s, \tag{2.7b}$$

with $\alpha > 0$ a penalty parameter that needs to be chosen sufficiently large to ensure stability [30, 37].

Boundedness and stability of a_h were proven in [30]. In particular, it was shown that there exists a constant $\alpha_0 > 0$ such that for $\alpha > \alpha_0$

$$a_h(\boldsymbol{v}_h, \boldsymbol{v}_h) \gtrsim \nu |||\boldsymbol{v}_h|||_1^2 \qquad \forall \boldsymbol{v}_h \in \boldsymbol{V}_h, \tag{2.8}$$

and that

$$\left|a_h(\boldsymbol{u}, \boldsymbol{v}_h)\right| \lesssim \nu |||\boldsymbol{u}|||_{1,*} |||\boldsymbol{v}_h|||_1 \qquad \forall \boldsymbol{u} \in V(h)\times\bar{V}(h) \text{ and } \forall \boldsymbol{v}_h \in \boldsymbol{V}_h. \tag{2.9}$$

Furthermore, stability of b_h was shown in [33]:

$$|||\boldsymbol{q}_h|||_Q \lesssim \sup_{\boldsymbol{v}_h\in\boldsymbol{V}_h} \frac{b_h(\boldsymbol{q}_h, v_h)}{|||\boldsymbol{v}_h|||_1} \qquad \forall \boldsymbol{q}_h \in \boldsymbol{Q}_h. \tag{2.10}$$

The well-posedness of the discrete Stokes problem (2.6) follows directly from the above stability results (see, for example, [3]).

Setting $\boldsymbol{q}_h = (\nabla \cdot u_h, 0) \in \boldsymbol{Q}_h$ in (2.6b) it is immediately clear that $\nabla \cdot u_h = 0$ pointwise on a cell. The EDG method, however, is not $H(\mathrm{div})$-conforming on Ω. This is because (2.6b) imposes only weak continuity of the normal component of the velocity across cell facets. The lack of $H(\mathrm{div})$-conformity was shown in [33, Remark 1] to be the reason that the EDG method is not pressure-robust; the velocity error has a dependence on $1/\nu$ times the pressure error,

$$\tag{2.11} |||\boldsymbol{u} - \boldsymbol{u}_h|||_1 \lesssim \inf_{\substack{\boldsymbol{v}_h \in \boldsymbol{V}_h \\ b_h(\boldsymbol{q}_h, v_h)=0\,\forall \boldsymbol{q}_h \in \boldsymbol{Q}_h}} |||\boldsymbol{u} - \boldsymbol{v}_h|||_{1,*} + \frac{1}{\nu} \inf_{\boldsymbol{q}_h \in \boldsymbol{Q}_h} |||\boldsymbol{p} - \boldsymbol{q}_h|||_Q.$$

In the remainder of this paper we modify the EDG method (2.6) to restore pressure-robustness.

3. Pressure-robustness.

In the continuous Stokes problem the velocity field is not affected by adding a gradient field to the body force. To see this, consider the continuous Stokes problem: find $u \in [H_0^1(\Omega)]^{\dim}$ and $p \in L_0^2(\Omega)$ such that

$$\tag{3.1a} \int_\Omega \nu \nabla u : \nabla v \,\mathrm{d}x - \int_\Omega p \nabla \cdot v \,\mathrm{d}x = \int_\Omega f \cdot v \,\mathrm{d}x \qquad \forall v \in \left[H_0^1(\Omega)\right]^{\dim},$$

$$\tag{3.1b} - \int_\Omega q \nabla \cdot u \,\mathrm{d}x = 0 \qquad \forall q \in L_0^2(\Omega).$$

By defining $V_0 := \{v \in [H_0^1(\Omega)]^{\dim} \;:\; \int_\Omega q \nabla \cdot v = 0 \;\forall q \in L_0^2(\Omega)\}$ we can formulate the following equivalent problem to (3.1): find $u \in V_0$ such that

$$\tag{3.2} \int_\Omega \nu \nabla u : \nabla v \,\mathrm{d}x = \int_\Omega f \cdot v \,\mathrm{d}x \quad \forall v \in V_0.$$

Changing the body force by a gradient field, i.e., changing f to $f + \nabla\psi$ with $\psi \in H^1(\Omega)$, we observe (using integration by parts) that

$$\tag{3.3} \int_\Omega \nu \nabla u : \nabla v \,\mathrm{d}x = \int_\Omega (f + \nabla\psi) \cdot v \,\mathrm{d}x = \int_\Omega f \cdot v \,\mathrm{d}x \quad \forall v \in V_0.$$

In other words, the irrotational part of the body force does not affect the velocity solution.

Many traditional finite element methods are not pressure-robust because the irrotational part of the body force is not L^2-orthogonal with discretely divergence-free vector fields [27]. This is true also for the EDG method (2.6). Indeed, define $V_{h,0} := \{v_h \in V_h \;:\; b_h(\boldsymbol{q}_h, v_h) = 0 \;\forall \boldsymbol{q}_h \in \boldsymbol{Q}_h\}$. Then an equivalent problem to (2.6) is given by the following: find $\boldsymbol{u}_h \in V_{h,0} \times \bar{V}_h$ such that

$$\tag{3.4} a_h(\boldsymbol{u}_h, \boldsymbol{v}_h) = \int_\Omega f \cdot v_h \,\mathrm{d}x \quad \forall \boldsymbol{v}_h \in V_{h,0} \times \bar{V}_h.$$

Adding a gradient field $\nabla\psi$, with $\psi \in H^1(\Omega)$, to the body force, we observe that for all $\boldsymbol{v}_h \in V_{h,0} \times \bar{V}_h$ it holds that

$$\tag{3.5} \begin{aligned} a_h(\boldsymbol{u}_h, \boldsymbol{v}_h) &= \int_\Omega (f + \nabla\psi) \cdot v_h \,\mathrm{d}x \\ &= \int_\Omega f \cdot v_h \,\mathrm{d}x - \sum_{K \in \mathcal{T}} \int_K \psi \nabla \cdot v_h \,\mathrm{d}x + \sum_{K \in \mathcal{T}} \int_{\partial K} \psi v_h \cdot n \,\mathrm{d}s. \end{aligned}$$

As we saw in subsection 2.3, if $v_h \in V_{h,0}$, then v_h is exactly divergence-free on a cell K, but v_h is not $H(\mathrm{div})$-conforming on Ω. We obtain

$$a_h(\boldsymbol{u}_h, \boldsymbol{v}_h) = \int_\Omega f \cdot v_h \,\mathrm{d}x + \sum_{K \in \mathcal{T}} \int_{\partial K} \psi v_h \cdot n \,\mathrm{d}s, \tag{3.6}$$

showing that the irrotational part of the body force now also changes the discrete velocity $\boldsymbol{u}_h$. If v_h were to have been $H(\mathrm{div})$-conforming on Ω, such as the HDG and EDG-HDG variants of (2.6) [33], then the last term in (3.6) would have vanished, and the discretization would be pressure-robust.

In the following sections we modify the EDG method to restore pressure-robustness. For this we require the following notation. The set of vertices is denoted by $\mathcal{V}$. For each vertex $V \in \mathcal{V}$ we define the vertex patch $\omega_V := \cup_{K: V \in \bar{K}} K \subset \Omega$ and the triangulation on the vertex patch $\mathcal{T}_V := \left\{K \in \mathcal{T} \ : \ K \cap \omega_V \neq \emptyset\right\}$. We denote by $\mathcal{F}_V$ the set of all interior facets in ω_V that are connected to V; hence $\mathcal{F}_V := \cup_{F: V \in \bar{F}} F$. Furthermore, $|\mathcal{T}_V|$ and $|\mathcal{F}_V|$ denote, respectively, the area of the vertex patch and the area of the interior skeleton.

3.1. A pressure-robust EDG method. To restore pressure-robustness of the EDG method (2.6), we follow an idea first introduced in [27] for the Crouzeix–Raviart finite element. Therein a reconstruction operator $\mathcal{R}$ is introduced that maps weakly divergence-free velocities onto exactly divergence-free velocities, i.e., velocities that are exactly divergence-free on a cell and $H(\mathrm{div})$-conforming. It is then proposed to replace the test function on the right-hand side of (2.6) by the reconstruction operator applied to the test function.

Several reconstruction operators have been introduced depending on the continuity properties of the pressure approximation. For discontinuous pressure approximations, the reconstruction operator can be defined locally on cells (see [27, 28]). For continuous pressure approximations, Lederer et al. [24] defined a reconstruction operator on vertex patches based on the ideas of the equilibrated a posteriori error estimator [4]. This reconstruction operator was successfully applied to the Taylor–Hood and mini elements.

To construct a reconstruction operator $\mathcal{R} : V_h \to V_h$ for the EDG method (2.6), in which the approximate trace pressure is continuous, we follow a similar approach as [24]. However, where in [24] a weakly divergence-free velocity is $H(\mathrm{div})$-conforming, but not exactly divergence-free on a cell, the opposite is true for the EDG method. As such, the reconstruction operator for the EDG method must be such that it compensates the normal jumps of a discrete velocity on cell-boundaries without changing the divergence of a discrete velocity on a cell. The definition and analysis of such an operator is postponed to subsection 3.3. To define a pressure-robust EDG method, it is sufficient for now to assume the following.

Assumption 3.1 (properties of an EDG reconstruction operator). There exists a reconstruction operator $\mathcal{R} : V_h \to V_h$ such that

(i) If $u_h \in V_h$ such that $b_h(\boldsymbol{q}_h, u_h) = 0$ for all $\boldsymbol{q}_h \in \boldsymbol{Q}_h$, then $\nabla \cdot \mathcal{R}(u_h) = 0$ pointwise on cells, $\mathcal{R}(u_h) \in H(\mathrm{div}, \Omega)$, and $\mathcal{R}(u_h) \cdot n = 0$ on $\partial\Omega$.

(ii) For all $u_h \in V_h$ we have

$$\left\|\mathcal{R}(u_h) - u_h\right\|_{L^2(\Omega)} \lesssim h |||u_h|||_1.$$

(iii) For $g \in [L^2(\Omega)]^{\dim}$ we have $(g, \mathcal{R}(u_h) - u_h)_{L^2(\Omega)} \lesssim |||g|||_{\mathrm{con},k} |||u_h|||_1$ with

$$|||g|||_{\mathrm{con},k} := \left(\sum_{V\in\mathcal{V}} h^2 \int_{\omega_V} (g - \Pi^{k-2}_{\omega_V} g)^2 \,\mathrm{d}x \right)^{1/2},$$

where $\Pi^{k-2}_{\omega_V}$ is the L^2-projection operator on polynomials of order $k-2$ on the vertex patch ω_V.

Remark 3.2. If $g \in [H^s(\Omega)]^{\dim}$ with $s \geq k-1$, then a standard scaling argument shows that

$$|||g|||_{\mathrm{con},k} \lesssim h^k \|g\|_{H^{k-1}(\Omega)}.$$

Let $\mathcal{R} : V_h \to V_h$ be a reconstruction operator that satisfies Assumption 3.1. We define the pressure-robust EDG method as the following: find $(\boldsymbol{u}_h, \boldsymbol{p}_h) \in \boldsymbol{V}_h \times \boldsymbol{Q}_h$ such that

$$a_h(\boldsymbol{u}_h, \boldsymbol{v}_h) + b_h(\boldsymbol{p}_h, v_h) = \int_\Omega f \cdot \mathcal{R}(v_h) \,\mathrm{d}x \qquad \forall \boldsymbol{v}_h \in \boldsymbol{V}_h, \tag{3.7a}$$

$$b_h(\boldsymbol{q}_h, u_h) = 0 \qquad \forall \boldsymbol{q}_h \in \boldsymbol{Q}_h. \tag{3.7b}$$

Since by item (i) of Assumption 3.1 $\mathcal{R}(v_h) \in H(\mathrm{div}, \Omega)$ is exactly divergence-free, it is clear that the irrotational part of the body force will not change the discrete velocity $\boldsymbol{u}_h$.

3.2. A priori error analysis. In this section we show optimal a priori velocity error estimates for the EDG method (3.7) that are independent of the pressure.

THEOREM 3.3 (pressure-robust a priori velocity error estimate). *Let* $(\boldsymbol{u}_h, \boldsymbol{p}_h) \in \boldsymbol{V}_h \times \boldsymbol{Q}_h$ *be the solution to* (3.7), *let* $(u, p) \in [H^2(\mathcal{T}) \cap H^1_0(\Omega)]^{\dim} \times L^2_0(\Omega)$ *be the exact solution to* (2.1), *and set* $\boldsymbol{u} = (u, u)$. *The following a priori error estimate holds:*

$$|||\boldsymbol{u} - \boldsymbol{u}_h|||_1 \lesssim \inf_{\substack{\boldsymbol{v}_h \in \boldsymbol{V}_h \\ b_h(\boldsymbol{q}_h, v_h) = 0\, \forall \boldsymbol{q}_h \in \boldsymbol{Q}_h}} |||\boldsymbol{u} - \boldsymbol{v}_h|||_{1,*} + |||\Delta u|||_{\mathrm{con},k}. \tag{3.8}$$

Proof. Let $\boldsymbol{v}_h = (v_h, \bar{v}_h) \in \boldsymbol{V}_h$ be an arbitrary test function such that $b_h(\boldsymbol{q}_h, v_h) = 0$ for all $\boldsymbol{q}_h \in \boldsymbol{Q}_h$, and let $\boldsymbol{w}_h := \boldsymbol{v}_h - \boldsymbol{u}_h$. By stability (2.8) and boundedness (2.9) of a_h we find

$$\begin{aligned} \nu |||\boldsymbol{w}_h|||_1^2 &\lesssim a_h(\boldsymbol{w}_h, \boldsymbol{w}_h) \\ &= a_h(\boldsymbol{v}_h - \boldsymbol{u}, \boldsymbol{w}_h) + a_h(\boldsymbol{u} - \boldsymbol{u}_h, \boldsymbol{w}_h) \\ &\lesssim \nu |||\boldsymbol{v}_h - \boldsymbol{u}|||_{1,*} |||\boldsymbol{w}_h|||_1 + a_h(\boldsymbol{u}, \boldsymbol{w}_h) - a_h(\boldsymbol{u}_h, \boldsymbol{w}_h). \end{aligned} \tag{3.9}$$

Consider the second term on the right-hand side of (3.9). Continuity of u and ∇u across element interfaces and integration by parts gives

(3.10)

$$\begin{aligned} a_h(\boldsymbol{u}, \boldsymbol{w}_h) &= \sum_{K\in\mathcal{T}} \int_K \nu \nabla u : \nabla w_h \,\mathrm{d}x + \sum_{K\in\mathcal{T}} \int_{\partial K} \nu \tfrac{\partial u}{\partial n} \cdot (\bar{w}_h - w_h) \,\mathrm{d}s \\ &= \sum_{K\in\mathcal{T}} \int_K -\nu \Delta u \cdot w_h \,\mathrm{d}x + \sum_{K\in\mathcal{T}} \int_{\partial K} \nu \tfrac{\partial u}{\partial n} \cdot \bar{w}_h \,\mathrm{d}s = (-\nu\Delta u, w_h)_{L^2(\Omega)}, \end{aligned}$$

where we used that $\bar{w}_h$ is single valued on element interfaces. Consider now the third term on the right-hand side of (3.9). Since $\boldsymbol{u}_h$ satisfies (3.7),

$$
\begin{aligned}
a_h(\boldsymbol{u}_h,\boldsymbol{w}_h) &= \int_\Omega f\cdot\mathcal{R}(w_h)\,\mathrm{d}x - b_h(\boldsymbol{p}_h,w_h) = \int_\Omega f\cdot\mathcal{R}(w_h)\,\mathrm{d}x \\
&= \int_\Omega (-\nu\Delta u+\nabla p)\cdot\mathcal{R}(w_h)\,\mathrm{d}x = (-\nu\Delta u,\mathcal{R}(w_h))_{L^2(\Omega)},
\end{aligned}
\tag{3.11}
$$

where we used integration by parts and item (i) of Assumption 3.1 for the last equality. Combining (3.9)–(3.11) and using item (ii) and item (iii) of Assumption 3.1 we find

$$
\begin{aligned}
\nu|||\boldsymbol{w}_h|||_1^2 &\lesssim \nu|||\boldsymbol{v}_h-\boldsymbol{u}|||_{1,*}|||\boldsymbol{w}_h|||_1 + (-\nu\Delta u, w_h-\mathcal{R}(w_h))_{L^2(\Omega)} \\
&\lesssim \nu|||\boldsymbol{v}_h-\boldsymbol{u}|||_{1,*}|||\boldsymbol{w}_h|||_1 + \nu\left(\sum_{V\in\mathcal{V}} h^2\int_{\omega_V}(\Delta u-\Pi_{\omega_V}^{k-2}\Delta u)^2\,\mathrm{d}x\right)^{1/2}|||\boldsymbol{w}_h|||_1 \\
&\lesssim \nu|||\boldsymbol{v}_h-\boldsymbol{u}|||_{1,*}|||\boldsymbol{w}_h|||_1 + \nu|||\Delta u|||_{\mathrm{con},k}|||\boldsymbol{w}_h|||_1.
\end{aligned}
$$

The result follows after dividing by $\nu|||\boldsymbol{w}_h|||_1$, noting that $\boldsymbol{v}_h$ is arbitrary, and a triangle inequality. ∎

Observe that unlike the velocity error estimate (2.11) for the discrete Stokes problem (2.6), the velocity error estimate (3.8) of the pressure-robust EDG method (3.7) does not depend on the pressure error. A consequence of Theorem 3.3 is the following result.

COROLLARY 3.4. *Let* $(u,p)\in[H^2(\mathcal{T})\cap H_0^1(\Omega)\cap H^{k+1}(\Omega)]^{\dim}\times H^k(\Omega)\cap L_0^2(\Omega)$ *be the exact solution to* (2.1), *and set* $\boldsymbol{u}=(u,u)$. *Then the solution* $(\boldsymbol{u}_h,\boldsymbol{p}_h)\in\boldsymbol{V}_h\times\boldsymbol{Q}_h$ *to* (3.7) *satisfies*

$$
|||\boldsymbol{u}-\boldsymbol{u}_h|||_1 \lesssim h^k\|u\|_{H^{k+1}(\mathcal{T})}.
$$

Proof. Let $\boldsymbol{v}_h=(I_{BDM}u,\Pi_{\mathcal{F}}u)\in\boldsymbol{V}_h$, where $I_{BDM}:[H^1(\Omega)]^{\dim}\to V_h$ is the usual Brezzi–Douglas–Marini (BDM) interpolation operator (see, for example, [14, Lemma 7]) and $\Pi_{\mathcal{F}}u$ is the L^2-projection into the facet velocity space. Since $\nabla\cdot I_{BDM}u=0$ the result follows by the approximation properties of the BDM interpolation operator and the L^2-projection (see [3]), Theorem 3.3, and Remark 3.2. ∎

3.3. An EDG-reconstruction operator. In this section we present an EDG reconstruction operator that satisfies the properties of Assumption 3.1. Its construction is based on the ideas of the equilibrated error estimator (see [4]).

To construct the EDG reconstruction operator we require the following spaces:

$$
\begin{aligned}
\Sigma_h^V &:= \left\{\tau_h\in[L^2(\omega_V)]^{\dim}:\tau_h\in[P_k(K)]^{\dim}\ \forall K\in\mathcal{T}_V \text{ and } \tau_h\cdot n=0 \text{ on } \partial\omega_V\right\}, \\
Q_h^V &:= \left\{q_h\in L^2(\omega_V)\ :\ q_h\in P_{k-1}(K)\ \forall K\in\mathcal{T}_V\right\}, \\
\bar{Q}_h^V &:= \left\{\bar{q}_h\in L^2(\mathcal{F}_V)\ :\ q_h\in P_k(F)\ \forall F\in\mathcal{F}_V\right\}, \\
\Lambda_h^V &:= \kappa_{x-V}([P_{k-3}(\omega_V)]^{\dim(\dim-1)/2}),
\end{aligned}
$$

where we note that Σ_h^V is the discontinuous BDM space on $\mathcal{T}_V$ of degree k with zero normal component on the boundary of the vertex patch ω_V. Furthermore, κ is the Koszul operator. For dim $=2$ with $x=(x_1,x_2)$ and for dim $=3$ with $x=(x_1,x_2,x_3)$ it is given by

$$
\begin{aligned}
&\kappa_x: L^2(\Omega)\to[L^2(\Omega)]^2, && \kappa_x:[L^2(\Omega)]^3\to[L^2(\Omega)]^3, \\
&\kappa_x(a):=\begin{pmatrix}-x_2\\ x_1\end{pmatrix}a, && \kappa_x(a):=x\times a.
\end{aligned}
$$

We note that the definition of the space Λ_h^V is motivated by the (Helmholtz-like) decomposition

$$[P^{k-2}(\omega_V)]^{\dim} = \nabla P^{k-1}(\omega_V) \oplus \kappa_{x-V}\left(\left[P_{k-3}(\omega_V)\right]^{\dim(\dim-1)/2}\right), \tag{3.12}$$

where the first term of the right-hand side is rotational-free and the second term is divergence-free; see, for example, [2, equation (3.11)]. Furthermore, we define the tensor space

$$\boldsymbol{Q}_h^V := \left\{Q_h^V \times \bar{Q}_h^V\right\}/\mathbb{R} = \left\{q_h, \bar{q}_h \in Q_h^V \times \bar{Q}_h^V : \sum_{K\in\mathcal{T}_V}\int_K q_h \,\mathrm{d}x + \sum_{F\in\mathcal{F}_V}\int_F \bar{q}_h \,\mathrm{d}s = 0\right\}.$$

3.3.1. Definition and analysis of a local problem. Let V be a vertex in the interior of Ω and $G^V(\cdot) \in \left(\boldsymbol{Q}_h^V\right)'$ be a given right-hand side (defined in subsection 3.3.2). We define the local problem: find $(\sigma_h^V, \boldsymbol{p}_h^V, \lambda_h^V) \in \Sigma_h^V \times \boldsymbol{Q}_h^V \times \Lambda_h^V$ such that

$$a_h^V(\sigma_h^V, \tau_h^V) + b_{1,h}^V(\boldsymbol{p}_h^V, \tau_h^V) + b_{2,h}^V(\lambda_h^V, \tau_h^V) = 0 \qquad \forall \tau_h^V \in \Sigma_h^V, \tag{3.13a}$$

$$b_{1,h}^V(\boldsymbol{q}_h^V, \sigma_h^V) = G^V(\boldsymbol{q}_h^V) \qquad \forall \boldsymbol{q}_h^V \in \boldsymbol{Q}_h^V, \tag{3.13b}$$

$$b_{2,h}^V(\mu_h^V, \sigma_h^V) = 0 \qquad \forall \mu_h^V \in \Lambda_h^V, \tag{3.13c}$$

where

$$a_h^V(\sigma_h^V, \tau_h^V) := \sum_{K\in\mathcal{T}_V}\int_K \sigma_h^V \cdot \tau_h^V \,\mathrm{d}x, \tag{3.14a}$$

$$b_{1,h}^V(\boldsymbol{q}_h^V, \sigma_h^V) := \sum_{K\in\mathcal{T}_V}\int_K \nabla\cdot\sigma_h^V q_h^V \,\mathrm{d}x + \sum_{F\in\mathcal{F}_V}\int_F [\![\sigma_h^V\cdot n]\!]\bar{q}_h^V \,\mathrm{d}s, \tag{3.14b}$$

$$b_{2,h}^V(\mu_h^V, \sigma_h^V) := \sum_{K\in\mathcal{T}_V}\int_K \sigma_h^V \cdot \mu_h^V \,\mathrm{d}x. \tag{3.14c}$$

Remark 3.5. In the definition of the local problems we assumed that the vertex V lies in the interior of the domain Ω. If V lies on the boundary of Ω, i.e., $V \in \partial\Omega$, we modify Σ_h^V to

$$\Sigma_h^V := \left\{\tau_h \in [L^2(\omega_V)]^{\dim} : \tau_h \in [P_k(K)]^{\dim},\ \forall K \in \mathcal{T}_V \text{ and } \tau_h\cdot n = 0 \text{ on } \partial\omega_V \setminus \partial\Omega\right\}.$$

Note that the local facet space $\overline{Q}_h^V$ now includes DOFs that are associated to facets F lying on the boundary $\partial\omega_V \cap \partial\Omega$. Hence, where the Dirichlet boundary conditions (in normal direction) of σ_h^V on $\partial\omega_V \setminus \partial\Omega$ are incorporated in the space Σ_h^V, the Dirichlet boundary conditions on $\partial\omega_V \cap \partial\Omega$ are incorporated in a weak sense in (3.13b) (see also Remark 3.8).

For the stability analysis of the local problem (3.13) we define the following mesh-dependent norms:

$$\|\tau_h^V\|^2_{\Sigma_h^V} := \|\tau_h^V\|^2_{L^2(\omega_V)} + h^2\|\nabla\cdot\tau_h^V\|^2_{L^2(\omega_V)} + h\,\|[\![\tau_h^V\cdot n]\!]\|^2_{L^2(\mathcal{F}_V)} \qquad \forall \tau_h^V \in \Sigma_h^V,$$

$$\|\boldsymbol{q}_h^V\|^2_{\boldsymbol{Q}_h^V} := \frac{1}{h^2}\|q_h^V\|^2_{L^2(\omega_V)} + \frac{1}{h}\|\bar{q}_h^V\|^2_{L^2(\mathcal{F}_V)} \qquad \forall \boldsymbol{q}_h^V \in \boldsymbol{Q}_h^V,$$

$$\|\mu_h^V\|_{\Lambda_h^V} := \|\mu_h^V\|_{L^2(\omega_V)} \qquad \forall \mu_h^V \in \Lambda_h^V.$$

THEOREM 3.6 (stability of (3.13)). *There exists a unique solution* $(\sigma_h^V, \boldsymbol{p}_h^V, \lambda_h^V) \in \Sigma_h^V \times \boldsymbol{Q}_h^V \times \Lambda_h^V$ *to problem* (3.13) *with the stability estimate*

$$\|\sigma_h^V\|_{\Sigma_h^V} + \|\boldsymbol{p}_h^V\|_{\boldsymbol{Q}_h^V} + \|\lambda_h^V\|_{\Lambda_h^V} \lesssim \|G^V\|_{(\boldsymbol{Q}_h^V)'}. \tag{3.15}$$

Proof. The proof is based on the theory of mixed saddle point problems (see [3, Chapter 4]); we need to prove kernel coercivity of the bilinear form $a_h^V(\cdot,\cdot)$ and the inf-sup condition of the constraints given by the bilinear forms $b_{1,h}^V(\cdot,\cdot)$ and $b_{2,h}^V(\cdot,\cdot)$.

Let $\sigma_h^V \in \Sigma_h^V$ such that $b_{1,h}^V(\boldsymbol{q}_h^V, \sigma_h^V) + b_{2,h}^V(\mu_h^V, \sigma_h^V) = 0$ for all $\boldsymbol{q}_h^V \in \boldsymbol{Q}_h^V$ and for all $\mu_h^V \in \Lambda_h^V$. Next, note that $(-\nabla\cdot\sigma_h^V, [\![\sigma_h^V \cdot n]\!]) \in \boldsymbol{Q}_h^V$ since integration by parts shows

$$-\sum_{K\in\mathcal{T}_V} \int_K \nabla\cdot\sigma_h^V \,\mathrm{d}x + \sum_{F\in\mathcal{F}_V} \int_F [\![\sigma_h^V \cdot n]\!] \,\mathrm{d}s = 0.$$

Choosing $\boldsymbol{q}_h^V = (-\nabla\cdot\sigma_h^V, [\![\sigma_h^V \cdot n]\!])$ and $\mu_h^V = 0$ in $b_{1,h}^V(\boldsymbol{q}_h^V, \sigma_h^V) + b_{2,h}^V(\mu_h^V, \sigma_h^V) = 0$ results in

$$\|\sigma_h^V\|^2_{\Sigma_h^V} = \|\sigma_h^V\|^2_{L^2(\omega_V)} = a_h^V(\sigma_h^V, \sigma_h^V), \tag{3.16}$$

proving kernel coercivity of $a_h^V(\cdot,\cdot)$.

We continue with the inf-sup condition of $b_{1,h}^V(\cdot,\cdot)$. To this end let $\boldsymbol{q}_h^V \in \boldsymbol{Q}_h^V$ be arbitrary. Using [4, Lemma 3 and Lemma 9] we find a function $\sigma_h^q \in \Sigma_h^V$ such that on each cell $K \in \mathcal{T}_V$ we have $-\nabla\cdot\sigma_h^q = q_h^V$, on all facets $F \in \mathcal{F}_V$ we have $[\![\sigma_h^q \cdot n]\!] = \bar{q}_h^V$, and $\sigma_h^q \in \Sigma_h^V$ satisfies the stability estimate $\|\sigma_h^q\|_{\Sigma_h^V} \lesssim \|\boldsymbol{q}_h\|_{\boldsymbol{Q}_h^V}$. Together these results prove the inf-sup condition

$$\inf_{\sigma_h^V\in\Sigma_h^V} \frac{b_{1,h}^V(\boldsymbol{q}_h^V, \sigma_h^V)}{\|\sigma_h^V\|_{\Sigma_h^V}} \gtrsim \|\boldsymbol{q}_h\|_{\boldsymbol{Q}_h^V}. \tag{3.17}$$

We next consider $b_{2,h}^V(\cdot,\cdot)$. Choose an arbitrary $\mu_h^V = \kappa_{x-V}(\zeta) \in \Lambda_h^V$ where $\zeta \in ([P_{k-3}(\omega_V)]^{\dim(\dim-1)/2})$, and set $\sigma_h^\mu = \mathrm{curl}(\phi_V\zeta)$, where ϕ_V is the corresponding linear hat function of the fixed vertex V. Since $\phi_V\zeta$ is a polynomial of order $k-2$ and since ϕ_V vanishes at the boundary $\partial\omega_V$, so that $\sigma_h^\mu \cdot n = 0$ on $\partial\omega_V$, we have $\sigma_h^\mu \in \Sigma_h^V$. (Here curl is the usual curl operator in three dimensions. In two dimensions it is defined as the rotated gradient, i.e., $\mathrm{curl} = (-\partial_{x_2}, \partial_{x_1})$.) Now note that $b_{1,h}(\boldsymbol{q}_h^V, \sigma_h^\mu) = 0$ for all test functions $\boldsymbol{q}_h^V \in \boldsymbol{Q}_h^V$ since the divergence of a curl is zero on $K \in \mathcal{T}_V$ and the normal jump disappears by properties of the discrete de Rham complex (see, for example, [3]). With the same steps as in the proof of [24, Theorem 12] we obtain the inf-sup condition (on the kernel of $b_{1,h}(\cdot,\cdot)$)

$$\inf_{\substack{\sigma_h^V\in\Sigma_h^V \\ b_{1,h}(\boldsymbol{q}_h^V, \sigma_h^\mu)=0, \forall \boldsymbol{q}_h^V\in\boldsymbol{Q}_h^V}} \frac{b_{2,h}^V(\mu_h^V, \sigma_h^\mu)}{\|\sigma_h^V\|_{\Sigma_h^V}} \gtrsim \|\mu_h^V\|_{\Lambda_h^V}.$$

The coupled inf-sup condition for $b_{1,h}+b_{2,h}$ now follows by application of [16, Theorem 3.1]. Together with the kernel coercivity (3.16) we conclude existence, uniqueness, and stability of (3.13). ∎

3.3.2. Definition and analysis of the EDG-reconstruction operator. In this section we define the EDG-reconstruction operator. To this end we first introduce an operator defined on vertex patches.

Let $V \in \mathcal{V}$ be an arbitrary vertex, and let $F \in \mathcal{F}_V$ be an arbitrary edge on the corresponding vertex patch of V. Furthermore, let $\bar{q}_h \in P^m(F)$ with $m = k, k-1$, let φ_i with $i = 0, \ldots, m$ be a Lagrangian basis of the polynomial space $P^m(F)$, and let ξ_i be the associated Lagrangian points. Then for $x \in F$ we can write $\bar{q}_h(x) = \sum_{i=0}^m c_i \varphi_i(x)$ where c_i are the related coefficients. We define the bubble projection $\mathbb{B}_F^V : P^m(F) \to P^m(F)$ as

$$\mathbb{B}_F^V(\bar{q}_h)(x) = \sum_{i=0}^m c_i \phi_V(\xi_i) \varphi_i(x).$$

The definition of the bubble projector $\mathbb{B}_F^V$ reads as a simple weighting of the coefficients c_i with the value of the hat function at the related Lagrangian point ξ_i. For the case $\dim = 2$, let V_o be the opposite vertex of V of F. By definition, $\mathbb{B}_F^V(\bar{q}_h)(V_o) = 0$, and we have the identity

$$\mathbb{B}_F^V(\bar{q}_h)(x) + \mathbb{B}_F^{V_o}(\bar{q}_h)(x) = \sum_{i=0}^m c_i(\phi_V(\xi_i) + \phi_{V_o}(\xi_i))\varphi_i(x) = \bar{q}_h(x). \tag{3.18}$$

For the case $\dim = 3$, let V_{o_1} and V_{o_2} be the opposite vertices of V of the triangle F, and let E_{12} be the edge connecting the vertices V_{o_1} and V_{o_2}. With the same arguments as above we have $\mathbb{B}_F^V(\bar{q}_h)|_{E_{12}} = 0$ and

$$\mathbb{B}_F^V(\bar{q}_h)(x) + \mathbb{B}_F^{V_{o_1}}(\bar{q}_h)(x) + \mathbb{B}_F^{V_{o_2}}(\bar{q}_h)(x) = \bar{q}_h(x). \tag{3.19}$$

Note that the definition for $\dim = 3$ equals the bubble projection on triangles defined in [24, section 4.1].

Now, let $u_h \in V_h$ be an arbitrary but fixed discrete velocity, and let σ_h^V be the solution to the local problem (3.13) defined on vertex patches with the following right-hand side:

$$G^V(\boldsymbol{q}_h) = \sum_{F \in \mathcal{F}_V} \int_F [\![u_h \cdot n]\!] \mathbb{B}_F^V \circ (\mathrm{id} - \Pi^0_{\mathcal{F}_V})(\bar{q}_h)\, \mathrm{d}s \quad \forall \boldsymbol{q}_h = (q_h, \bar{q}_h) \in \boldsymbol{Q}_h, \tag{3.20}$$

where $\Pi^0_{\mathcal{F}_V}$ is the projection onto constants on $\mathcal{F}_V$, i.e.,

$$\Pi^0_{\mathcal{F}_V}(q) = \frac{1}{|\mathcal{F}_V|} \sum_{F \in \mathcal{F}_V} \int_F q \, \mathrm{d}s \quad \forall q \in L^2(\mathcal{F}_V).$$

THEOREM 3.7 (properties of the local solutions). *Let $u_h \in V_h$, let $V \in \mathcal{V}$ be arbitrary but fixed, and let σ_h^V be the solution to* (3.13) *with the right-hand side defined by* (3.20)*. Furthermore, let σ_h^V be trivially extended to $\Omega \setminus \omega_V$ by zero.*

(i) *For all $(q_h, \bar{q}_h^d) \in Q_h \times \bar{Q}_h^d$ we have*

$$(\nabla \cdot \sigma_h^V, q_h)_{L^2(\mathcal{T})} + ([\![\sigma_h^V \cdot n]\!], \bar{q}_h^d)_{L^2(\mathcal{F})} = (\mathbb{B}_F^V \circ (\mathrm{id} - \Pi^0_{\mathcal{F}_V})([\![u_h \cdot n]\!]), \bar{q}_h^d)_{L^2(\mathcal{F})}.$$

(ii) *We have $\|\sigma_h^V\|_{\Sigma_h^V} \lesssim \sqrt{h}\, \|[\![u_h \cdot n]\!]\|_{L^2(\mathcal{F}_V)}$.*

(iii) *If $b_h(\boldsymbol{q}_h, u_h) = 0$ for all $\boldsymbol{q}_h \in \boldsymbol{Q}_h$, then $(\sigma_h^V, \eta_h)_{L^2(\omega_V)} = 0$ for all $\eta_h \in P^{k-2}(\omega_V)$.*

Proof. We start with the proof of item (i). We first show that the solution σ_h^V satisfies

$$b_{1,h}^V((c,c),\sigma_h^V) = G^V((c,c)) \quad \forall c \in \mathbb{R}.$$

To show this we first note that the left-hand side vanishes by integration by parts, i.e., $b_{1,h}((c,c),\sigma_h^V) = 0$. Next, note that $\Pi^0_{\mathcal{F}_V}(c) = c$, and so the right-hand side also vanishes.

Now let $(q_h, \bar{q}_h^d) \in Q_h \times \bar{Q}_h^d$ be arbitrary, and set $\boldsymbol{q}_h^V = (q_h|_{\omega_V}, \bar{q}_h^d|_{\omega_V})$, i.e., the restriction on the vertex patch. We define the constant

$$c := \frac{1}{|\mathcal{T}_V| + |\mathcal{F}_V|}\left(\sum_{K\in\mathcal{T}_V}\int_K q_h|_{\omega_V}\,\mathrm{d}x + \sum_{F\in\mathcal{F}_V}\int_F \bar{q}_h^d|_{\omega_V}\,\mathrm{d}s\right)$$

and write $\boldsymbol{q}_h^V = (q_h|_{\omega_V} - c, \bar{q}_h^d|_{\omega_V} - c) + (c,c)$. The first term of the right-hand side is an element of $\boldsymbol{Q}_h^V$, and so with the above findings and (3.13b) we observe that

$$b_{1,h}^V(\boldsymbol{q}_h^V,\sigma_h^V) = G^V(\boldsymbol{q}_h^V).$$

Using that σ_h^V is zero on $\Omega \setminus \omega_V$ we then find that

$$\begin{aligned}(\nabla\cdot\sigma_h^V, q_h)_{L^2(\mathcal{T})} + ([\![\sigma_h^V\cdot n]\!],\bar{q}_h)_{L^2(\mathcal{F})} &= b_{1,h}^V(\boldsymbol{q}_h^V,\sigma_h^V) = G^V(\boldsymbol{q}_h^V)\\ &= (\mathbb{B}_F^V\circ(\mathrm{id}-\Pi^0_{\mathcal{F}_V})([\![u_h\cdot n]\!]),\bar{q}_h)_{L^2(\mathcal{F}_V)}.\end{aligned}$$

We next prove item (ii). Using the stability result (3.15) this follows by definition of the dual norm,

$$\begin{aligned}\|\sigma_h^V\|_{\Sigma_h^V} \lesssim \|G^V\|_{(\boldsymbol{Q}_h^V)'} &:= \sup_{0\neq \boldsymbol{r}_h^V\in\boldsymbol{Q}_h^V}\frac{G^V(\boldsymbol{r}_h^V)}{\|\boldsymbol{r}_h^V\|_{\boldsymbol{Q}_h^V}}\\ &\le \sup_{0\neq \boldsymbol{r}_h^V\in\boldsymbol{Q}_h^V}\frac{\|\mathbb{B}_F^V\circ(\mathrm{id}-\Pi^0_{\mathcal{F}_V})[\![u_h\cdot n]\!]\|_{L^2(\mathcal{F}_V)}\,\|\bar{r}_h^V\|_{L^2(\mathcal{F}_V)}}{\|\boldsymbol{r}_h^V\|_{\boldsymbol{Q}_h^V}}\\ &\le \sqrt{h}\,\|\mathbb{B}_F^V\circ(\mathrm{id}-\Pi^0_{\mathcal{F}_V})[\![u_h\cdot n]\!]\|_{L^2(\mathcal{F}_V)}\\ &\le \sqrt{h}\,\|[\![u_h\cdot n]\!]\|_{L^2(\mathcal{F}_V)} + \sqrt{h}\,\|\Pi^0_{\mathcal{F}_V}[\![u_h\cdot n]\!]\|_{L^2(\mathcal{F}_V)}\\ &\lesssim \sqrt{h}\,\|[\![u_h\cdot n]\!]\|_{L^2(\mathcal{F}_V)},\end{aligned}$$

where we used continuity of $\Pi^0_{\mathcal{F}_V}$ and the bubble projector since the weighting of the coefficient lies in $[0,1]$.

Finally, we prove item (iii). Let $\eta_h \in P^{k-2}(\omega_V)$ be arbitrary. Using decomposition (3.12) we find polynomials $\theta \in P^{k-1}(\omega_V)$ and $\zeta \in ([P_{k-3}(\omega_V)]^{\dim(\dim-1)/2})$ such that

$$\eta_h = \nabla\theta + \kappa_{x-V}(\zeta).$$

Note that θ can be chosen such that $(\theta,\theta) \in \boldsymbol{Q}_h^V$ since the above decomposition includes only the gradient of θ. Using (3.13c), we note that $(\sigma_h^V, \kappa_{x-V}(\zeta))_{L^2(\omega_V)} = 0$. Next, using integration by parts,

$$\begin{aligned}(\sigma_h^V,\nabla\theta)_{\omega_V} &= b_{1,h}^V((\theta,\theta),\sigma_h^V) = G^V((\theta,\theta))\\ &= \sum_{F\in\mathcal{F}_V}\int_F [\![u_h\cdot n]\!]\mathbb{B}_F^V\circ(\mathrm{id}-\Pi^0_{\mathcal{F}_V})\theta\,\mathrm{d}s = 0,\end{aligned}$$

since $\mathbb{B}_F^V\circ(\mathrm{id}-\Pi^0_{\mathcal{F}_V})\theta$ is an element of $\bar{Q}_h$. ∎

Remark 3.8. We noted in Remark 3.5 that Dirichlet boundary conditions (in normal direction) of σ_h^V on $\partial\omega_V \cap \partial\Omega$ are incorporated in a weak sense. Indeed, from (3.13b), item (i) of Theorem 3.7, and $\sigma_h^V \cdot n \in \overline{Q}_h^d$ we find

$$\sigma_h^V \cdot n = \mathbb{B}_F^V \circ (\mathrm{id} - \Pi^0_{\mathcal{F}_V})(u_h \cdot n) \quad \text{on } \partial\omega_V \cap \partial\Omega.$$

We are now able to define a reconstruction operator that satisfies the properties of Assumption 3.1.

LEMMA 3.9. *Let $u_h \in V_h$, and let σ_h^V be the solution to* (3.13) *with the right-hand side defined by* (3.20) *for an arbitrary vertex $V \in \mathcal{V}$. The reconstruction operator $\mathcal{R} : V_h \to V_h$ defined by*

$$\mathcal{R}(u_h) := u_h - \sigma_h \quad \textit{with} \quad \sigma_h := \sum_{V \in \mathcal{V}} \sigma_h^V$$

satisfies the properties of Assumption 3.1.

Proof. We first prove that the reconstruction operator satisfies item (i) of Assumption 3.1. Let $u_h \in V_h$ such that $b_h(\boldsymbol{r}_h, u_h) = 0$ for all $\boldsymbol{r}_h \in \boldsymbol{Q}_h$. Now let $(q_h, \bar{q}_h^d) \in Q_h \times \bar{Q}_h^d$ be arbitrary; then

$$\begin{aligned}
&\sum_{K \in \mathcal{T}} \int_K \nabla \cdot \mathcal{R}(u_h) q_h \,\mathrm{d}x + \sum_{F \in \mathcal{F}} \int_F [\![\mathcal{R}(u_h) \cdot n]\!] \bar{q}_h^d \,\mathrm{d}s \\
&\qquad = \sum_{K \in \mathcal{T}} \int_K \nabla \cdot u_h q_h \,\mathrm{d}x + \sum_{F \in \mathcal{F}} \int_F [\![u_h \cdot n]\!] \bar{q}_h^d \,\mathrm{d}s \\
&\qquad\quad - \sum_{K \in \mathcal{T}} \int_K \nabla \cdot \sigma_h q_h \,\mathrm{d}x - \sum_{F \in \mathcal{F}} \int_F [\![\sigma_h \cdot n]\!] \bar{q}_h^d \,\mathrm{d}s.
\end{aligned} \tag{3.21}$$

Consider the last two terms on the right-hand side. By definition of σ_h,

$$\begin{aligned}
&- \sum_{K \in \mathcal{T}} \int_K \nabla \cdot \sigma_h q_h \,\mathrm{d}x - \sum_{F \in \mathcal{F}} \int_F [\![\sigma_h \cdot n]\!] \bar{q}_h^d \,\mathrm{d}s \\
&\quad = - \sum_{K \in \mathcal{T}} \sum_{V \in K} \int_K \nabla \cdot \sigma_h^V q_h \,\mathrm{d}x - \sum_{F \in \mathcal{F}} \sum_{V \in F} \int_F [\![\sigma_h^V \cdot n]\!] \bar{q}_h^d \,\mathrm{d}s \\
&\quad = \sum_{V \in \mathcal{V}} \left(- \sum_{K \in \mathcal{T}_V} \int_K \nabla \cdot \sigma_h^V q_h \,\mathrm{d}x - \sum_{F \in \mathcal{F}_V} \int_F [\![\sigma_h^V \cdot n]\!] \bar{q}_h^d \,\mathrm{d}s \right) \\
&\quad = \sum_{V \in \mathcal{V}} \left(- \sum_{F \in \mathcal{F}_V} \int_F \mathbb{B}_F^V \circ (\mathrm{id} - \Pi^0_{\mathcal{F}_V})([\![u_h \cdot n]\!]) \bar{q}_h^d \,\mathrm{d}s \right) \\
&\quad = \sum_{V \in \mathcal{V}} \left(- \sum_{F \in \mathcal{F}_V} \int_F \mathbb{B}_F^V([\![u_h \cdot n]\!]) \bar{q}_h^d \,\mathrm{d}s + \sum_{F \in \mathcal{F}_V} \int_F [\![u_h \cdot n]\!] \mathbb{B}_F^V \circ \Pi^0_{\mathcal{F}_V}(\bar{q}_h^d) \,\mathrm{d}s \right),
\end{aligned}$$

where we used item (i) of Theorem 3.7 for the third equality and that $\mathbb{B}_F^V \circ \Pi^0_{\mathcal{F}_V}$ is a symmetric self adjoint operator for the fourth equality. Since u_h is discretely divergence-free and $\mathbb{B}_F^V \circ \Pi^0_{\mathcal{F}_V}(\bar{q}_h) \in \bar{Q}_h$, the second sum on the right-hand side vanishes. Therefore, using (3.19),

$$
\begin{aligned}
(3.22)\qquad -\sum_{K\in\mathcal{T}}\int_K \nabla\cdot\sigma_h q_h \,\mathrm{d}x - \sum_{F\in\mathcal{F}}\int_F [\![\sigma_h\cdot n]\!]\bar{q}_h^d \,\mathrm{d}s
&= \sum_{V\in\mathcal{V}}\sum_{F\in\mathcal{F}_V} -\int_F \mathbb{B}_F^V([\![u_h\cdot n]\!])\bar{q}_h^d \,\mathrm{d}s \\
&= \sum_{F\in\mathcal{F}}\sum_{V\in F} -\int_F \mathbb{B}_F^V([\![u_h\cdot n]\!])\bar{q}_h^d \,\mathrm{d}s = -\sum_{F\in\mathcal{F}}\int_F [\![u_h\cdot n]\!]\bar{q}_h^d \,\mathrm{d}s.
\end{aligned}
$$

Combining (3.21) and (3.22) we find that

$$
\begin{aligned}
&\sum_{K\in\mathcal{T}}\int_K \nabla\cdot\mathcal{R}(u_h) q_h \,\mathrm{d}x + \sum_{F\in\mathcal{F}}\int_F [\![\mathcal{R}(u_h)\cdot n]\!]\bar{q}_h^d \,\mathrm{d}s \\
&\quad= \sum_{K\in\mathcal{T}}\int_K \nabla\cdot u_h q_h \,\mathrm{d}x + \sum_{F\in\mathcal{F}}\int_F [\![u_h\cdot n]\!]\bar{q}_h^d \,\mathrm{d}s - \sum_{F\in\mathcal{F}}\int_F [\![u_h\cdot n]\!]\bar{q}_h^d \,\mathrm{d}s = 0,
\end{aligned}
$$

where we used that $\nabla\cdot u_h$ vanishes in each cell. Now, since $\nabla\cdot\mathcal{R}(u_h)\in Q_h$ and $[\![\mathcal{R}(u_h)\cdot n]\!]\in\bar{Q}_h^d$, we conclude that $\mathcal{R}(u_h)\in H(\mathrm{div},\Omega)$ and $\nabla\cdot\mathcal{R}(u_h)=0$. The homogeneous normal Dirichlet boundary conditions follow by Remark 3.8.

To prove that the reconstruction operator satisfies item (ii) of Assumption 3.1 we use item (ii) from Theorem 3.7:

$$
\begin{aligned}
\|\mathcal{R}(u_h)-u_h\|_{L^2(\Omega)}^2 = \|\sigma_h\|_{L^2(\Omega)}^2 &\le \sum_{V\in\mathcal{V}}\|\sigma_h^V\|_{L^2(\omega_V)}^2 \\
&\le \sum_{V\in\mathcal{V}}\|\sigma_h^V\|_{\Sigma_h^V}^2 \lesssim \sum_{V\in\mathcal{V}} h\,\|[\![u_h\cdot n]\!]\|_{L^2(\mathcal{F}_V)}^2 \le h^2 |\!|\!| u_h |\!|\!|_1^2.
\end{aligned}
$$

The result follows after taking the square root on both sides.

Finally, we prove item (iii) of Assumption 3.1. Let $g\in[L^2(\Omega)]^{\dim}$ be arbitrary. Using item (iii) and item (ii) from Theorem 3.7 we find that

$$
\begin{aligned}
(g,\mathcal{R}(u_h)-u_h)_{L^2(\Omega)} &= \sum_{V\in\mathcal{V}}\int_{\omega_V}\sigma_h^V\cdot g\,\mathrm{d}x \\
&= \sum_{V\in\mathcal{V}}\int_{\omega_V}\sigma_h^V\cdot(g-\Pi_{\omega_V}^{k-2}g)\,\mathrm{d}x \\
&\le \sum_{V\in\mathcal{V}}\left[\left(\frac{1}{h}\|\sigma_h^V\|_{L^2(\omega_V)}\right)\left(h^2\int_{\omega_V}(g-\Pi_{\omega_V}^{k-2}g)^2\,\mathrm{d}x\right)^{1/2}\right] \\
&\le \left(\sum_{V\in\mathcal{V}}\frac{1}{h^2}\|\sigma_h^V\|_{L^2(\omega_V)}^2\right)^{1/2}\left(\sum_{V\in\mathcal{V}}h^2\int_{\omega_V}(g-\Pi_{\omega_V}^{k-2}g)^2\,\mathrm{d}x\right)^{1/2} \\
&\le \left(\sum_{V\in\mathcal{V}}\frac{1}{h}\|[\![u_h\cdot n]\!]\|_{\mathcal{F}_V}^2\right)^{1/2}\left(\sum_{V\in\mathcal{V}}h^2\int_{\omega_V}(g-\Pi_{\omega_V}^{k-2}g)^2\,\mathrm{d}x\right)^{1/2} \\
&\le |\!|\!| u_h |\!|\!|_1\left(\sum_{V\in\mathcal{V}}h^2\int_{\omega_V}(g-\Pi_{\omega_V}^{k-2}g)^2\,\mathrm{d}x\right)^{1/2},
\end{aligned}
$$

concluding the proof. ∎

We remark that the reconstruction operator defined in Lemma 3.9 can easily be implemented in existing EDG codes for the Stokes problem since it is applied only to the right-hand side of the discretization (3.7). The left-hand side matrices of (2.6) and (3.7) are *identical*.

4. Numerical tests. In this section we present two and three dimensional numerical examples that demonstrate that the modified EDG discretization (3.7) with the reconstruction operator defined in Lemma 3.9 results in a pressure-robust discretization of the Stokes equations. All numerical examples have been implemented in the higher-order finite element library Netgen/NGSolve [34, 35]. We remark that the EDG method (2.6) can be implemented directly in the Netgen/NGSolve library. A C++ extension was written to implement the reconstruction operator that is required for the modified EDG method (3.7).

We study the Stokes problem (2.1) on $\Omega := [0,1]^{\dim}$. For $\dim = 2$ we set the body force f such that the exact solution is given by

$$u = \operatorname{curl}(\xi) \quad \text{and} \quad p = x_1^5 + x_2^5 - 1/3,$$

where $\xi = x_1^2(x_1-1)^2 x_2^2(x_2-1)^2$, while for $\dim = 3$ the body force is such that the exact solution is given by

$$u = \operatorname{curl}((\xi,\xi,\xi)) \quad \text{and} \quad p = x_1^5 + x_2^5 + x_3^5 - 1/2,$$

where $\xi = x_1^2(x_1-1)^2 x_2^2(x_2-1)^2 x_3^2(x_3-1)^2$.

In this section we denote the discrete velocity solution obtained by the EDG method (2.6) by u_h and the discrete velocity solution obtained by the modified EDG method (3.7) by $u_h^\star$. We furthermore define $e_h = u - u_h$ and $e_h^\star = u - u_h^\star$.

For the two dimensional test case we plot, in Figure 4.1 and Figure 4.2, respectively, the L^2-norm and H^1-seminorm (the L^2-norm of the gradient) of e_h and $e_h^\star$. We compute the solution for polynomial orders $k = 2,3,4$ and for both $m = k$ and $m = k-1$ in (2.3). We fix the viscosity to $\nu = 10^{-6}$.

From both figures we first observe optimal rates of convergence for all methods. We also observe that $u_h^\star$ is not affected by the choice of m. However, the choice of m does affect u_h, as we discuss next.

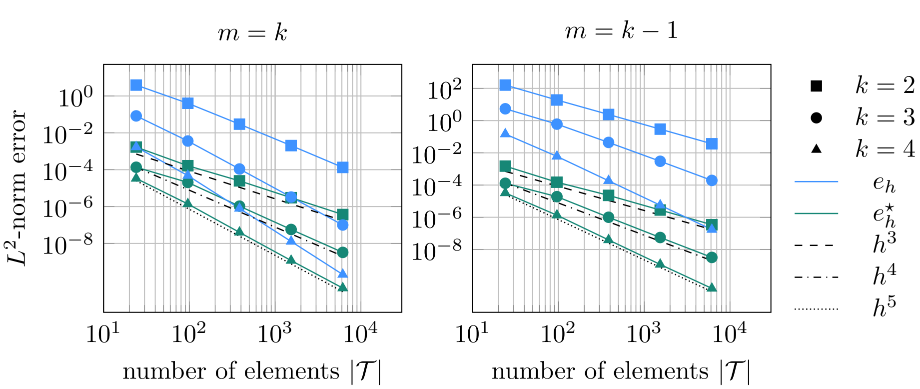

FIG. 4.1. *Two dimensional test case as described in section 4 using $\nu = 10^{-6}$. We plot the L^2-norm error of the velocity, against the number of elements in the mesh, for polynomial degrees $k = 2,3,4$. Here $e_h = u - u_h$ and $e_h^\star = u - u_h^\star$ with u_h the discrete velocity solution to the EDG method (2.6) and $u_h^\star$ the discrete velocity solution to the modified EDG method (3.7). The solutions are computed both for $m = k$ in (2.3) (left) and when $m = k-1$ (right).*

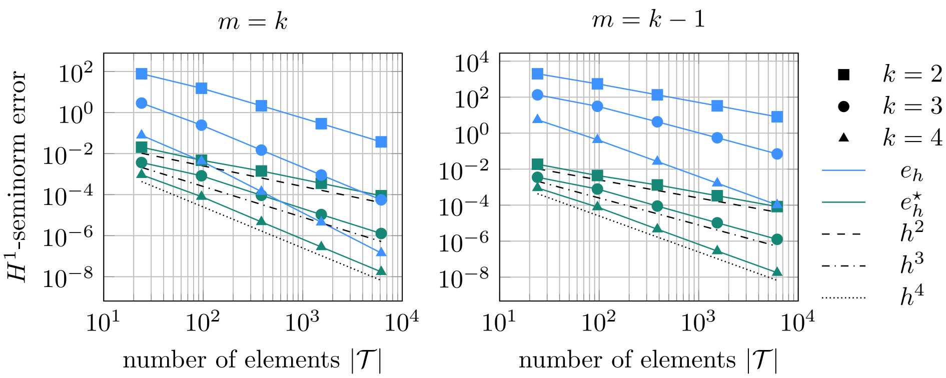

FIG. 4.2. *Two dimensional test case as described in section* 4 *using* $\nu = 10^{-6}$. *We plot the* H^1*-seminorm error of the velocity, against the number of elements in the mesh, for polynomial degrees* $k = 2, 3, 4$. *Here* $e_h = u - u_h$ *and* $e_h^\star = u - u_h^\star$ *with* u_h *the discrete velocity solution to the EDG method* (2.6) *and* $u_h^\star$ *the discrete velocity solution to the modified EDG method* (3.7). *The solutions are computed both for* $m = k$ *in* (2.3) *(left) and when* $m = k - 1$ *(right).*

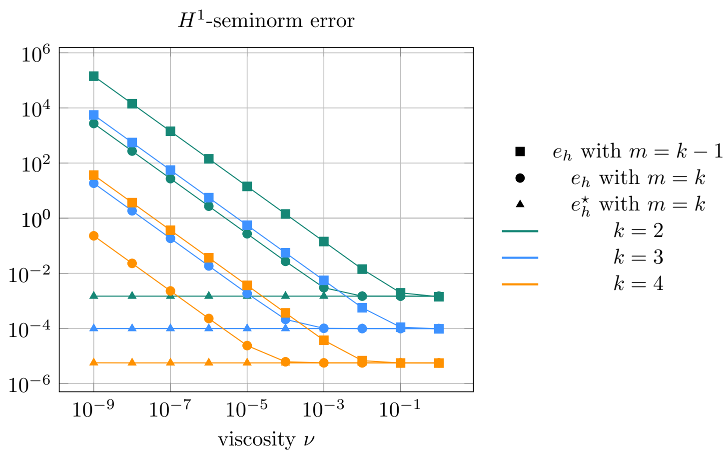

FIG. 4.3. *Two dimensional test case as described in section* 4 *using a fixed mesh with* $|\mathcal{T}| = 230$ *elements. We plot the* H^1*-seminorm error of the velocity against varying viscosities* $\nu = 1, \ldots, 10^{-9}$ *for polynomial degrees* $k = 2, 3, 4$. *Here* $e_h = u - u_h$ *and* $e_h^\star = u - u_h^\star$ *with* u_h *the discrete velocity solution to the EDG method* (2.6) *and* $u_h^\star$ *the discrete velocity solution to the modified EDG method* (3.7). *The solutions* u_h *are computed both for* $m = k$ *and* $m = k - 1$.

For the case $m = k - 1$ we observe that $u_h^\star$ is significantly more accurate than u_h when $\nu = 10^{-6}$; $e_h^\star$ is 10^3–10^5 times smaller (depending on k) than e_h in both the L^2-norm and in the H^1-seminorm.

When $m = k$ we note that e_h is approximately 10^2 times smaller than when $m = k-1$. We conjecture that this is due to a better enforcement of continuity of the normal component of the velocity. As such, when $m = k$, u_h is "closer" to an $H(\mathrm{div})$-conforming velocity than when $m = k - 1$, mitigating the role of the pressure-error in (2.11). Due to u_h being more accurate when $m = k$, and because the accuracy of $u_h^\star$ does not seem to depend on m, we observe that $u_h^\star$ is "only" 10–10^2 times more accurate (depending on k) than u_h.

We now vary the viscosity from $\nu = 1$ to $\nu = 10^{-9}$ and plot the H^1-seminorm on a fixed mesh with $|\mathcal{T}| = 230$ triangles for polynomial orders $k = 2, 3, 4$ in Figure 4.3. We observe that $e_h^\star$ is not affected by ν, thereby verifying Corollary 3.4. As

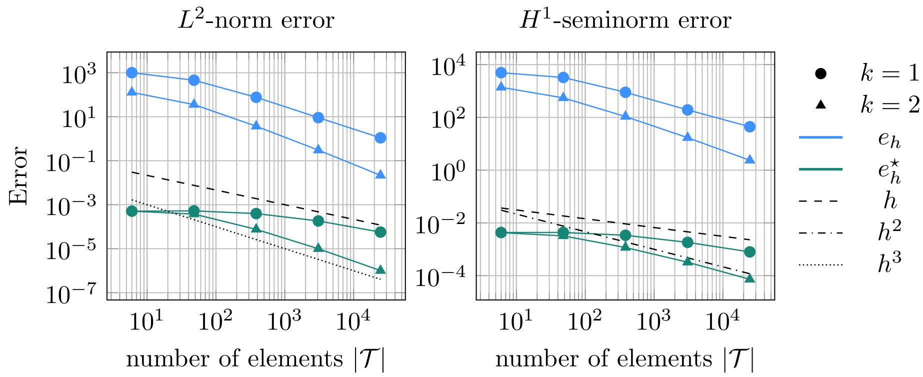

FIG. 4.4. *Three dimensional test case as described in section 4 using $\nu = 10^{-6}$. We plot the L^2-norm (left) and H^1-seminorm (right) errors of the velocity, against the number of elements in the mesh, for polynomial degrees $k = 1, 2$. Here $e_h = u - u_h$ and $e_h^\star = u - u_h^\star$ with u_h the discrete velocity solution to the EDG method* (2.6) *and $u_h^\star$ the discrete velocity solution to the modified EDG method* (3.7). *The solutions are computed using $m = k$ in* (2.3).

expected from (2.11), the accuracy of u_h deteriorates as viscosity decreases. Furthermore, in agreement with our previous observations, the solution u_h with $m = k$ is approximately 10^2 times more accurate than with $m = k - 1$.

In Figure 4.4 we plot the L^2-norm and H^1-seminorm of the error of the discrete velocity for the three dimensional test case. We again set $\nu = 10^{-6}$ and compute the solution for polynomial orders $k = 1, 2$. We consider only the case $m = k$ since the EDG method with $m = k - 1$ is not defined for $k = 1$. We draw the same conclusions as in the two dimensional test case, namely, optimal rates of convergence for all methods and a pressure-robust discrete velocity approximation when using the modified EDG method.

5. Conclusions. We introduced a new reconstruction operator that restores pressure-robustness for an EDG discretization of the Stokes equations. We have shown that this reconstruction operator can be constructed locally on vertex patches and needs to be applied only to the right-hand-side vector, allowing for easy implementation in existing codes. Furthermore, by an a priori error analysis, we showed that the velocity errors converge optimally. Numerical examples in two and three dimensions support our analysis.

REFERENCES

[1] D. N. ARNOLD, F. BREZZI, AND M. FORTIN, *A stable finite element for the Stokes equations*, Calcolo, 21 (1984), pp. 337–344, https://doi.org/10.1007/BF02576171.

[2] D. N. ARNOLD, R. S. FALK, AND R. WINTHER, *Finite element exterior calculus, homological techniques, and applications*, Acta Numer., 15 (2006), pp. 1–155, https://doi.org/10.1017/S0962492906210018.

[3] D. BOFFI, F. BREZZI, AND M. FORTIN, *Mixed Finite Element Methods and Applications*, Springer Ser. Comput. Math. 44, Springer Verlag-Berlin, 2013.

[4] D. BRAESS AND J. SCHÖBERL, *Equilibrated residual error estimator for edge elements*, Math. Comp., 77 (2008), pp. 651–672, https://doi.org/10.1090/S0025-5718-07-02080-7.

[5] B. COCKBURN, J. GOPALAKRISHNAN, AND R. LAZAROV, *Unified hybridization of discontinuous Galerkin, mixed, and continuous Galerkin methods for second order elliptic problems*, SIAM J. Numer. Anal., 47 (2009), pp. 1319–1365, https://doi.org/10.1137/070706616.

[6] B. Cockburn, G. Kanschat, and D. Schötzau, *A note on discontinuous Galerkin divergence-free solutions of the Navier–Stokes equations*, J. Sci. Comput., 31 (2007), pp. 61–73, https://doi.org/10.1007/s10915-006-9107-7.

[7] M. Crouzeix and P. A. Raviart, *Conforming and nonconforming finite element methods for solving the stationary Stokes equations* I, ESAIM Math. Model. Numer. Anal., 7 (1973), pp. 33–75.

[8] D. Frerichs and C. Merdon, *Divergence-Preserving Reconstructions on Polygons and a Really Pressure-Robust Virtual Element Method for the Stokes Problem*, arXiv e-prints, 2020, https://arxiv.org/abs/2002.01830.

[9] G. Fu, *An explicit divergence-free DG method for incompressible flow*, Comput. Methods Appl. Mech. Engrg., 345 (2019), pp. 502–517, https://doi.org/10.1016/j.cma.2018.11.012.

[10] J. Gopalakrishnan, P. L. Lederer, and J. Schöberl, *A mass conserving mixed stress formulation for the Stokes equations*, IMA J. Numer. Anal., 40 (2020), pp. 1838–1874, https://doi.org/10.1093/imanum/drz022.

[11] J. Gopalakrishnan, P. L. Lederer, and J. Schöberl, *A mass conserving mixed stress formulation for Stokes flow with weakly imposed stress symmetry*, SIAM J. Numer. Anal., 58 (2020), pp. 706–732, https://doi.org/10.1137/19M1248960.

[12] J. Guzmán and M. Neilan, *Conforming and divergence-free Stokes elements in three dimensions*, IMA J. Numer. Anal., 34 (2014), pp. 1489–1508, https://doi.org/10.1093/imanum/drt053.

[13] J. Guzmán and M. Neilan, *Conforming and divergence-free Stokes elements on general triangular meshes*, Math. Comp., 83 (2014), pp. 15–36, https://doi.org/10.1090/S0025-5718-2013-02753-6.

[14] P. Hansbo and M. G. Larson, *Discontinuous Galerkin methods for incompressible and nearly incompressible elasticity by Nitsche's method*, Comput. Methods Appl. Mech. Engrg., 191 (2002), pp. 1895–1908, https://doi.org/10.1016/S0045-7825(01)00358-9.

[15] P. Hood and C. Taylor, *Navier–Stokes equations using mixed interpolation*, in Finite Element Methods in Flow Problems, J. T. Oden, R. H. Gallagher, O. C. Zienkiewicz, and C. Taylor, eds., University of Alabama in Huntsville Press, 1974, pp. 121–132.

[16] J. S. Howell and N. J. Walkington, *Inf-sup conditions for twofold saddle point problems*, Numer. Math., 118 (2011), pp. 663–693, https://doi.org/10.1007/s00211-011-0372-5.

[17] V. John, A. Linke, C. Merdon, M. Neilan, and L. G. Rebholz, *On the divergence constraint in mixed finite element methods for incompressible flows*, SIAM Rev., 59 (2017), pp. 492–544, https://doi.org/10.1137/15M1047696.

[18] G. Kanschat and N. Sharma, *Divergence-conforming discontinuous Galerkin methods and C^0 interior penalty methods*, SIAM J. Numer. Anal., 52 (2014), pp. 1822–1842, https://doi.org/10.1137/120902975.

[19] R. J. Labeur and G. N. Wells, *A Galerkin interface stabilisation method for the advection–diffusion and incompressible Navier–Stokes equations*, Comput. Methods Appl. Mech. Engrg., 196 (2007), pp. 4985–5000, https://doi.org/10.1016/j.cma.2007.06.025.

[20] R. J. Labeur and G. N. Wells, *Energy stable and momentum conserving hybrid finite element method for the incompressible Navier–Stokes equations*, SIAM J. Sci. Comput., 34 (2012), pp. A889–A913, https://doi.org/10.1137/100818583.

[21] P. L. Lederer, *A Mass Conserving Mixed Stress Formulation for Incompressible Flows*, PhD thesis, Technical University of Vienna, Vienna, Austria, 2019.

[22] P. L. Lederer, C. Lehrenfeld, and J. Schöberl, *Hybrid discontinuous Galerkin methods with relaxed H(div)-conformity for incompressible flows. Part* I, SIAM J. Numer. Anal., 56 (2018), pp. 2070–2094, https://doi.org/10.1137/17M1138078.

[23] P. L. Lederer, C. Lehrenfeld, and J. Schöberl, *Hybrid discontinuous Galerkin methods with relaxed H(div)-conformity for incompressible flows. Part* II, ESAIM Math. Model. Numer. Anal., 53 (2019), pp. 503–522, https://doi.org/10.1051/m2an/2018054.

[24] P. L. Lederer, A. Linke, C. Merdon, and J. Schöberl, *Divergence-free reconstruction operators for pressure-robust Stokes discretizations with continuous pressure finite elements*, SIAM J. Numer. Anal., 55 (2017), pp. 1291–1314, https://doi.org/10.1137/16M1089964.

[25] C. Lehrenfeld and J. Schöberl, *High order exactly divergence-free hybrid discontinuous Galerkin methods for unsteady incompressible flows*, Comput. Methods Appl. Mech. Engrg., 307 (2016), pp. 339–361, https://doi.org/10.1016/j.cma.2016.04.025.

[26] A. Linke, *A divergence-free velocity reconstruction for incompressible flows*, C. R. Math. Acad. Sci. Paris, 350 (2012), pp. 837–840, https://doi.org/10.1016/j.crma.2012.10.010.

[27] A. Linke, *On the role of the Helmholtz decomposition in mixed methods for incompressible flows and a new variational crime*, Comput. Methods Appl. Mech. Engrg., 268 (2014), pp. 782–800, https://doi.org/10.1016/j.cma.2013.10.011.

[28] A. Linke, G. Matthies, and L. Tobiska, *Robust arbitrary order mixed finite element methods for the incompressible Stokes equations with pressure independent velocity errors*, ESAIM Math. Model. Numer. Anal., 50 (2016), pp. 289–309, https://doi.org/10.1051/m2an/2015044.

[29] A. Linke and C. Merdon, *Pressure-robustness and discrete Helmholtz projectors in mixed finite element methods for the incompressible Navier–Stokes equations*, Comput. Methods Appl. Mech. Engrg., 311 (2016), pp. 304–326, https://doi.org/10.1016/j.cma.2016.08.018.

[30] S. Rhebergen and G. N. Wells, *Analysis of a hybridized/interface stabilized finite element method for the Stokes equations*, SIAM J. Numer. Anal., 55 (2017), pp. 1982–2003, https://doi.org/10.1137/16M1083839.

[31] S. Rhebergen and G. N. Wells, *A hybridizable discontinuous Galerkin method for the Navier–Stokes equations with pointwise divergence-free velocity field*, J. Sci. Comput., 76 (2018), pp. 1484–1501, https://doi.org/10.1007/s10915-018-0671-4.

[32] S. Rhebergen and G. N. Wells, *Preconditioning of a hybridized discontinuous Galerkin finite element method for the Stokes equations*, J. Sci. Comput., 77 (2018), pp. 1936–1952, https://doi.org/10.1007/s10915-018-0760-4.

[33] S. Rhebergen and G. N. Wells, *An embedded-hybridized discontinuous Galerkin finite element method for the Stokes equations*, Comput. Methods Appl. Mech. Engrg., 358 (2020), 112619 https://doi.org/10.1016/j.cma.2019.112619.

[34] J. Schöberl, *NETGEN An advancing front 2D/3D-mesh generator based on abstract rules*, Computing and Visualization in Science, 1 (1997), pp. 41–52.

[35] J. Schöberl, *C++11 implementation of finite elements in NGSolve*, Tech. Report ASC Report 30/2014, Institute for Analysis and Scientific Computing, Vienna University of Technology, Vienna, Austria, 2014, https://www.asc.tuwien.ac.at/~schoeberl/wiki/publications/ngs-cpp11.pdf.

[36] L. R. Scott and M. Vogelius, *Conforming finite element methods for incompressible and nearly incompressible continua*, in Large-Scale Computations in Fluid Mechanics, Part 2 (La Jolla, CA, 1983), Lectures in Appl. Math. 22,, AMS, Providence, RI, 1985, pp. 221–244.

[37] G. N. Wells, *Analysis of an interface stabilized finite element method: The advection-diffusion-reaction equation*, SIAM J. Numer. Anal., 49 (2011), pp. 87–109, https://doi.org/10.1137/090775464.